

A critical dimension for the stability of perfect fluid spheres of radiation

John Hammersley*

*Department of Mathematical Sciences,
Durham University, South Road, Durham DH1 3LE UK*

Abstract

An analysis of radiating perfect fluid models with asymptotically AdS boundary conditions is presented. Such scenarios consist of a spherical gas of radiation (a “star”) localised near the centre of the spacetime due to the confining nature of the AdS potential. We consider the variation of the total mass of the star as a function of the central density, and observe that for large enough dimensionality, the mass increases monotonically with the density. However in the lower dimensional cases, oscillations appear, indicating that the perfect fluid model of the star is becoming unrealistic. We find the critical dimension separating these two regimes to be eleven.

1 Introduction

There are numerous effects in physics which are dependent on the dimension of the spacetime in which they live, and concepts which have mathematically simple models when restricted to one or two dimensions may become intractably complex as the dimensionality increases. Furthermore, in some situations there is a sharp contrast in the behaviour of the system when the number of dimensions passes above or below a certain “critical dimension”. In the field of general relativity there are already some instances of such dimension dependent phenomena; for example, the Gregory-Laflamme instability [1, 2] of black strings, and the work of Belinsky, Khalatnikov and Lifshitz (BKL) [3] and its extensions [4, 5, 6], where the dynamics of a spacetime in the vicinity of a cosmological singularity were studied. In the latter case they found that the general behaviour of the relevant Einstein solutions changed from “chaotic” in the low dimensional cases to non-chaotic in higher dimensions. It is this extra complexity and appearance of a critical dimension which is discovered in the work presented here.

* John.Hammersley@dunelm.org.uk

The issue of dimensionality has become of even greater importance over the past few decades, with the theories of hidden dimensions first postulated by Kaluza [7] resurfacing in the quest for unification and a Theory of Everything. Originally it was hoped one extra dimension would be sufficient; with the advent of string theory and its subsequent developments this was then expanded to twenty six in the late 1960's as a consistency requirement for bosonic strings, before being reduced back down to ten with the introduction of supersymmetry in the 1980's. The idea of holography also has its roots in dimensionality, and its most famous form, that of Maldacena [8], states a relation between string theory on a five-dimensional anti-de Sitter space, and a four-dimensional conformal field theory. Much work (see [9] for a review) has followed investigating spacetimes and conformal field theories of varying dimension and complexity.

Here we present an analysis into the stability of radiating perfect fluid spheres in an asymptotically anti-de Sitter spacetime. Due to the confining nature of the AdS potential, the spheres of radiation are self-gravitating, and thus we shall refer to them as “stars” in much of the following, although this is mainly used as a conveniently brief label, as it is only a toy-model approximation to a star at best.

We begin by giving the equations for a such a model in d -dimensions, before analysing the behaviour of the star's total mass. We consider the variation of the total mass as a function of the central density, and observe that for large enough dimensionality, the mass increases monotonically with the density. However in the lower dimensional cases, oscillations appear (this was originally noted in the $d = 5$ case in [10]), indicating that the perfect fluid model of the star is becoming unrealistic. We numerically find the critical dimension separating these two regimes to be 11.0 (to three significant figures), and give an explicit relation, (11), between the spacetime dimension d and the “saturation density” ρ_c , see section 3.1. The existence of local maxima at critical central densities (saturation points) in the lower dimensional cases indicates the appearance of instabilities in the model of the star, and point to unrealistic effects developing for $\rho_0 > \rho_c$. We also provide a numerical analysis of the behaviour at large central density, in particular the self-similar behaviour that appears in dimension $d < d_c$; several parameters of our numerical model are then also determined analytically from a dynamical systems analysis of the behaviour, where we consider the expansion about a fixed point of the zero-cosmological constant solution.¹

The outline of the paper is as follows: we begin with a brief recap on perfect fluid models in general dimension in section 2. In section 3 we introduce the total mass as a function of the central density, analyse the progression of the saturation point with increasing dimension, and present the best fit formula, (11), which gives a value for the critical dimension. We also present further numerical results for

¹This dynamical systems analysis (section 4) was suggested after correspondence with V. Vaganov, who also considered the behaviour of self-gravitating radiation in AdS_d in [11]. Work simultaneously conducted by P. H. Chavanis also found the critical dimension described here, via an alternative route, in his comprehensive study of relativistic stars with a linear equation of state, [12] (see the note following the discussion for more details).

the behaviour of the total mass at large central densities. In section 4 we give a dynamical systems analysis, following the methods in [11] and [13], which yields analytical expressions for several of the numerical results of the previous section. Finally, we conclude with a discussion of the results in section 5.

2 Perfect fluid models

Consider a general static, spherically symmetric d -dimensional AdS spacetime with metric:

$$ds^2 = -k(r)dt^2 + h(r)dr^2 + r^2 d\Omega_{d-2}^2 \quad (1)$$

By considering a perfect fluid of a gas of radiation, one can obtain implicit expressions for $k(r)$ and $h(r)$ for a simple model of a “star” geometry. For a perfect fluid we have that the stress tensor is of the form:

$$T_{ab} = \rho(r)u_a u_b + P(r)(g_{ab} + u_a u_b) \quad (2)$$

where u^a is the d -velocity of a co-moving gas, and upon which we impose the further constraint that the matter be purely radiating; this sets $\rho(r) = (d-1)P(r)$ as it requires that T_{ab} be traceless. One obtains the required metric by solving Einstein’s equation: $G_{ab} + \Lambda g_{ab} = 8\pi G_d T_{ab}$, with the above stress tensor and a negative cosmological constant, as follows. The relevant components of Einstein’s equations in general dimension d are given by:

$$G_{rr} = \left(\frac{d-2}{2}\right) \frac{(d-3)(k(r) - k(r)h(r)) + rk'(r)}{r^2 k(r)} = \left(\frac{\rho(r)}{d-1} + \frac{(d-1)(d-2)}{2R^2}\right) h(r) \quad (3)$$

$$G_{tt} = k(r) \left(\frac{d-2}{2}\right) \frac{(d-3)(h^2(r) - h(r)) + rh'(r)}{r^2 h^2(r)} = \left(\rho(r) + \frac{(d-1)(d-2)}{2R^2}\right) k(r) \quad (4)$$

where we have used that $\Lambda = -(d-1)(d-2)/(2R^2)$, $P(r) = \rho(r)/(d-1)$, and set $8\pi G_d \equiv 1$ for convenience². We can infer the form of $h(r)$ from (4), as the $k(r)$ dependence cancels, and we find that $h(r)$ is given by:

$$h(r) = \left(1 + \frac{r^2}{R^2} - \frac{m(r)}{r^{d-3}}\right)^{-1} \quad (5)$$

where $m(r)$ is a mass function³ related to the density via:

$$m(r) = \frac{2}{d-2} \int_0^r \rho(\acute{r}) \acute{r}^{d-2} d\acute{r} \quad (6)$$

²In the numerical results presented shortly we also set $R = 1$; we include it here to ease comparison with the dynamical systems analysis of the $\Lambda = 0$ ($R = \infty$) case given in section 4.

³Note that the mass function used here is a rescaling of the actual mass; a constant factor from the integral over the angular directions does not appear in our definition of $m(r)$ due to our definition of $h(r)$.

In order to specify a form for $k(r)$, we recall the energy-momentum conservation equation, $\nabla_\mu T^{\mu\nu} = 0$, which for a general perfect fluid without the radiation condition gives:

$$P'(r) + \frac{k'(r)}{2k(r)}(P(r) + \rho(r)) = 0 \quad (7)$$

which can be re-arranged to give

$$k(r) = \left(\frac{\rho_\infty}{\rho(r)} \right)^{2/d} \quad (8)$$

in the radiation case, where we have introduced ρ_∞ , which is the leading coefficient of $\rho(r)$ at large r , and is given by $\rho_\infty \approx \rho(r)r^d$ as $r \rightarrow \infty$. Substituting $h(r)$ from (5) into (3) and eliminating $k'(r)/k(r)$ using (7) then gives an equation in terms of $m(r)$, $\rho(r)$ and $\rho'(r)$,

$$\frac{(d-3)}{r^2} \left(1 - \frac{1}{1 + \frac{r^2}{R^2} - \frac{m(r)}{r^{d-3}}} \right) - \frac{2\rho'(r)}{r\rho(r)d} = \frac{2\rho(r) + (d-1)^2(d-2)/R^2}{(d-1)(d-2) \left(1 + \frac{r^2}{R^2} - \frac{m(r)}{r^{d-3}} \right)} \quad (9)$$

which couples with our equation for $m'(r)$:

$$m'(r) = \frac{2}{d-2} \rho(r) r^{d-2} \quad (10)$$

to give a pair of ODEs. For specified dimension d , these allow the geometry of the spacetime to be numerically generated when they are combined with the relevant boundary conditions: $m(0) = 0$ and $\rho(0) = \rho_0$. The condition $\rho(0) = \rho_0$ specifies the central density of the gas, and we have that for fixed R , ρ_0 is the single free parameter of the system (pure AdS is recovered when $\rho_0 = 0$).

3 Total mass as a function of central density

Whilst mathematically one can work with this perfect fluid setup in any number of dimensions (including non-integer ones), one would also like to consider the appropriateness of doing so, given that we wish to use the geometry as the setup for a toy model of a star. In other words, is there any significant change in behaviour as the dimensionality of the model is altered. A particular quantity of interest in analysing the stability of the model is the total mass M of the star, and as we have just seen, the mass and density profiles of our gas of radiation are determined by a single parameter: the central density of the gas, ρ_0 .

To avoid possible instabilities such as those considered in the asymptotically flat case (in four dimensions) in [14], one would expect the total mass to increase monotonically with ρ_0 . One could also expect the total mass to be bounded from above by some maximum value, analogous to the $4d$ asymptotically flat case where

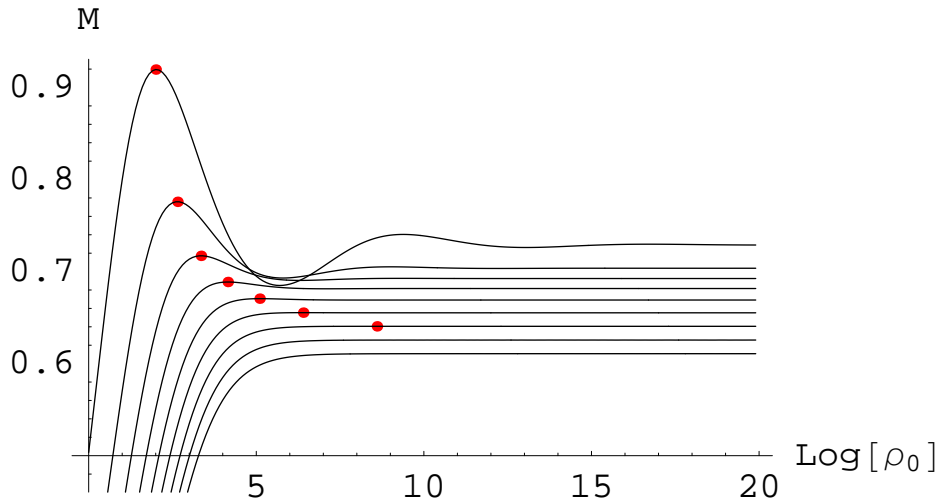


Fig. 1: Total mass vs density for the radiating perfect fluid model in various dimensions, from $d = 4$ (top curve) through to $d = 12$ (bottom curve). The saturation point for each dimension is indicated by the red dots; these correspond to the maximum value of the total mass in the relevant dimension, at the critical density ρ_c (see section 3.1). For d large, there is no local maximum and hence no finite saturation point; in these cases, the maximum total mass is given by the asymptotic value, η_d .

for a fixed size R_{star} , the maximum possible mass such a star can have is given by $M_{max} = 4R_{star}/9$, a result found by Buchdahl in 1959 [15].⁴

In our scenarios the total mass is indeed bounded from above, however, this maximum is not always the asymptotic value of the total mass at large density. Although we observe that as $\rho_0 \rightarrow \infty$ we have $M(\rho_0) \rightarrow \eta_d$, where η_d is some finite constant dependent on the dimension d (see section 3.2 below for more details), what we do not find in all cases is the total mass approaching this constant monotonically, see figure 1. When the dimensionality is low, there are sizable oscillations about the final value η_d before the curve settles down (see figure 2), as was noted in the $d = 5$ case in [10], and in other similar scenarios, e.g. [18], and the star’s maximum mass is given by some value greater than η_d . As the dimension is increased, however, these oscillations become less pronounced, and for d sufficiently high they disappear altogether, see figure 3.

Ideally one would like to analytically determine the dependence of the shape of the curve on both the dimension d and the density ρ_0 , however, due to the complexity of the equations, the exact behaviour must be computed numerically. One can nevertheless use this data to construct models of the various features of the star’s behaviour: for example, in section 3.2 below, we give an analysis of the

⁴For further edification, note that this equality coincides with the Buchdahl-Bondi limit, usually written in the form $R/M = 9/4$, which is the lowest radius to which the Schwarzschild geometry can be embedded (in Euclidean space). For more detail see e.g. [16, 17].

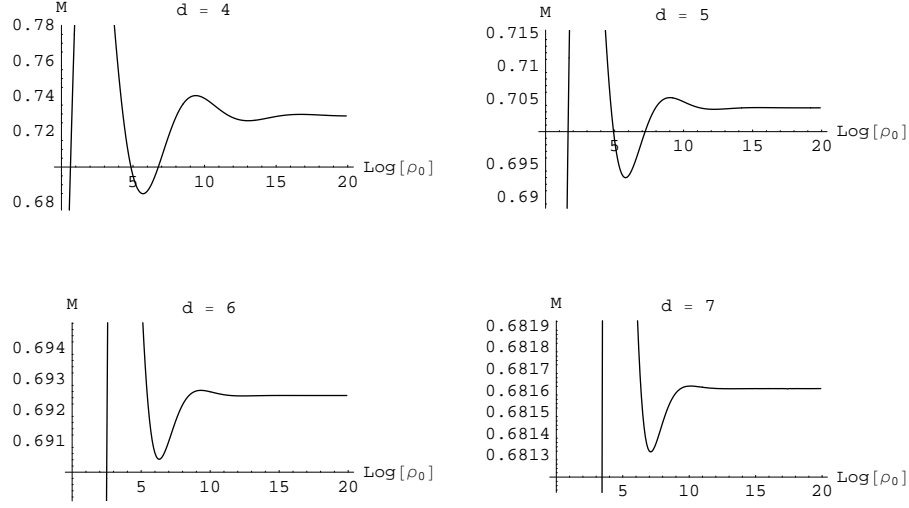


Fig. 2: The oscillations in the total mass M : as the central density ρ_0 is increased, M does not simply increase monotonically towards its final value η_d . Instead, it reaches a larger maximum before undergoing damped oscillations towards η_d . Note that the amplitude of the oscillations becomes smaller as the dimensionality d is increased.

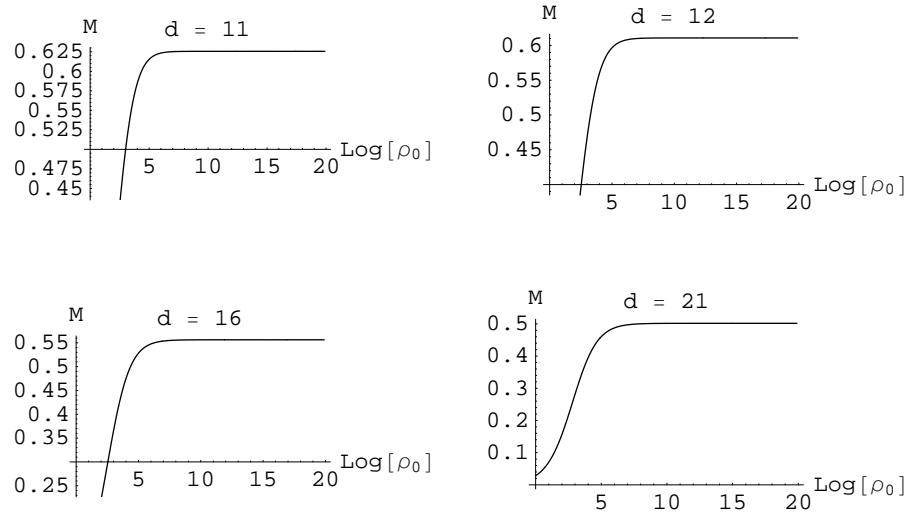


Fig. 3: For larger d , there are no oscillations in the total mass: M is now a monotonic function of the central density ρ_0 , and its maximum is also its asymptotic value as $\rho_0 \rightarrow \infty$, namely η_d .

total mass at large ρ_0 (where it approaches a constant, dependent on d) in different dimensions.

One particularly interesting feature is the appearance of the turning points in the total mass seen in figure 2, and specifically the locations of the local maxima in different dimensions. One can see from the figures that as the dimensionality is increased, the appearance of the first maximum moves to larger ρ_0 ; by analysing this progression one can obtain a remarkably simple relation which immediately gives a value for the critical dimension, above which the oscillations do not exist, and hence the total mass is a monotonic function of ρ_0 .

3.1 A critical dimension

The saturation point, ρ_c , which we define as being the location of the first local maximum when increasing ρ_0 , can be seen to progress to larger and larger ρ_0 as the dimension d is increased, see figure 1. What we wish to determine is whether this saturation point appears for all dimension d (for sufficiently large ρ_0), or whether there is a cut-off dimension, d_c , such that for larger d , there is no local maximum and hence no saturation point. Figure 4 shows how the saturation point varies with dimension; numerical analysis then finds (to 3 significant figures) that this behaviour is given by the following model:

$$\log \rho_c \approx 0.500 d + \frac{5.75}{\sqrt{11.0 - d}} - 2.20 \quad (11)$$

which gives a critical dimension $d_c = 11.0$.⁵ What is perhaps rather surprising is the simplicity of (11): not only do we have a critical dimension appearing so clearly, the overall dependence on d is remarkably simple, and the co-efficient of the linear term appears to be exactly one half.

As we shall see in section 4, the value of the critical dimension can also be determined by an analytical consideration of the radiating perfect fluid system with zero cosmological constant (i.e. in the limit $R \rightarrow \infty$). Although such a solution is singular at $r = 0$, and has infinite mass, by confining the radiation to finite sized box one can obtain finite mass solutions. The features determined in this configuration can be related to equivalent behaviour in the asymptotically anti-de Sitter case (where the (finite) mass is confined by the AdS potential), and indeed exact values for certain parameters can also be computed. This same analysis is not restricted to the star geometries considered here, it can be used with any linear equation of state [11], or even more generally [13]. Before giving the analysis for our case of perfect fluid radiation, however, we firstly present further numerical results.

⁵As mentioned earlier, correspondence with V. Vaganov and P. H. Chavanis suggested that the critical dimension in the radiating perfect fluid case is very close to (but not exactly) eleven, and this is indeed the case as we see in the dynamical systems analysis approach in section 4, where we obtain a value complementary to the numerical estimate of 11.0 given here. Interestingly, the exact value of $d_c = 11$ appears in the case of Newtonian isothermal spheres, as noticed by Sire and Chavanis in 2002 [19].

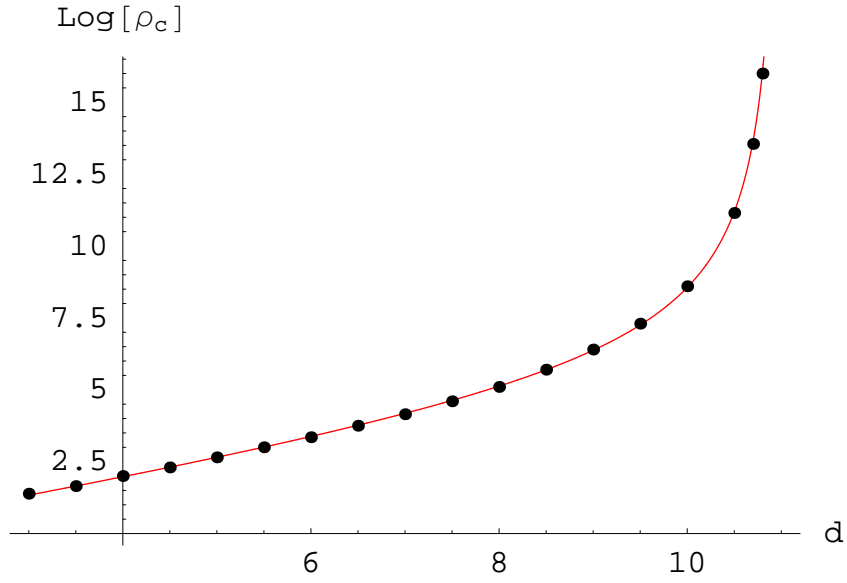


Fig. 4: The change in the saturation point ρ_c with increasing dimension d . The points plotted are the calculated values for the saturation point for the star model in the corresponding dimension, the red best fit line is the curve given by (11). The divergent behaviour as d approaches eleven indicates that for $d > 11$ there is no saturation point, and hence no apparent instability in the perfect fluid model of the “star”.

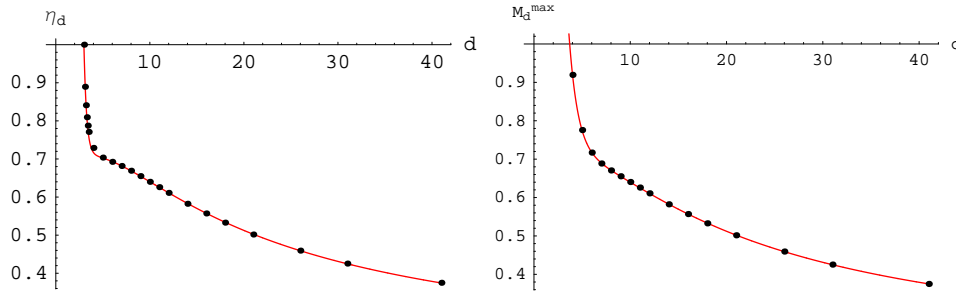


Fig. 5: The plot on the left shows η_d for various dimensions, with the approximation given in (12) shown in red. The data points are all at integer values for the dimension, with the addition of points at $d = 3.1, 3.2, \dots, 3.5$ to highlight the behaviour of the curve at low d . The righthand plot shows the behaviour of M_d^{\max} ; this is identical to that of η_d for $d \geq 11$, however for $d < 11$, the maximum is given by the value of the total mass at the saturation point, ρ_c . The best fit approximation (red curve) for each is simple in terms of its d dependence, and provides a good fit over a large range of d .

3.2 Total mass at large ρ_0

In addition to considering the variation of the saturation point for the star with dimension, one can also investigate the asymptotic behaviour of M as ρ_0 becomes large. As mentioned in section 3, at large ρ_0 , the value of the total mass tends to a constant, η_d , which is then only dependent on the dimension; the value of this constant decreases as d increases. The values are plotted in figure 5 and despite the complicated appearance of the plot, a remarkably close fit for all dimensions is given by:

$$\eta_d \approx 0.716 + \exp[9.85 - 3.72d] - \exp\left[-0.603 - \frac{20.3}{d}\right] \quad (12)$$

which is also shown in the figure. Checks show that the function continues to give accurate predictions for larger d , and although there is perhaps slightly more complicated behaviour for $d \sim 4$, we do not attempt to investigate this further here⁶; despite the relative compactness of the expression, there is little intuitive origin for any of the constants involved. Nonetheless, it is impressive that the behaviour of the mass at large ρ_0 can be expressed in such simple powers of the dimension.

One can perform a similar analysis of the behaviour of the maximum value of the total mass as the dimension increases; the results are also shown in figure 5. For $d > 11$, the maximum total mass corresponds to the asymptotic value, η_d , however, for lower dimension, the maximum is given by the mass at the saturation point. A

⁶Whilst in the dynamical systems analysis (section 4) the $d = 3$ case (where we have $\eta_3 = 1$) needs considering separately, as there is different asymptotic behaviour involved due to the non-dynamical nature of gravity in such a scenario (see [20] for example), we find that we can include it both here (in the analysis of η_d) and also in our earlier result for the critical dimension (see section 3.1).

d	α_d	β_d	μ_d	ν_d
3.1	0.305	0.184	8.33	0.66
4	0.383	0.371	8.44	0.86
5	0.400	0.601	9.35	0.98
6	0.415	0.825	10.3	1.03
7	0.431	1.03	11.4	1.07

Table 1: Numerical estimates for α_d , β_d , μ_d and ν_d (to three significant figures) for the model of the total mass given in (14) .

good fit to the curve is given by:

$$M_d^{max} \approx 0.712 + \exp[2.74 - 1.07d] - \exp\left[-0.592 - \frac{20.5}{d}\right] \quad (13)$$

which differs (significantly) from (12) only in the second term; this was to be expected, as the curves differ only at low d . Whilst there is little apparent significance about the values of the numerical constants involved in the expression, we have again produced a fit with a relatively simple dependence on d which gives accurate predictions for M_d^{max} over a large range of dimensions.

Although the form of the fit used in equations (12) and (13) was chosen primarily because it gave such a close fit to the data, it would be interesting to study possible reasons for expecting the observed dependence on dimension, although we do not pursue this further here. What we do now examine in more detail, is the oscillatory behaviour, which can be considered both numerically and analytically.

3.3 Self-similarity analysis for $d < 11$

Another interesting feature of the plots of the total mass seen in figures 1 and 2 is the self-similarity exhibited by the oscillatory behaviour as $\rho_0 \rightarrow \infty$. A numerical analysis of the periodicity and damping of the oscillations seen for $3 < d < 11$ leads us to propose the following model for the total mass:

$$M_d(\rho_0) \approx \eta_d + \alpha_d \exp[-\beta_d \log(\rho_0)] \cos[\mu_d - \nu_d \log(\rho_0)] \quad (14)$$

which gives a good approximation for the behaviour in the region $\rho_0 > \rho_c$. In (14), η_d is the asymptotic value of the mass discussed above, and the four parameters α_d , β_d , μ_d and ν_d are constants dependent only on the dimension d . Approximate values for these constants for $d = 3.1, 4, 5, 6$ and 7 are given in Table 1.

Although the values given in table 1 are only approximate, we nonetheless see interesting dependencies on d emerging. For example, β_d appears to increase roughly linearly with dimension ($\beta_d \approx 0.22d - 0.51$), as do α_d and μ_d for $d \geq 4$. We will see below in the dynamical systems analysis how this linear behaviour of β_d on d is only an approximation to the true behaviour, and the same analysis also provides exact values for the parameter ν_d . This analytical analysis also confirms the form of the fit used in the numerical approximation derived above.

4 Dynamical systems analysis

By considering the behaviour of the system of coupled ODEs given in section 2 in the limit $R \rightarrow \infty$, we can obtain analytical results for some of the interesting features of the radiating perfect fluid star geometries described above. The analysis presented here follows that detailed in both [11] and [13], where it is given in more general settings; by focusing on the radiation case (where $\rho(r) = (d-1)P(r)$) we can give a good explanation of why the numerical behaviour seen above is so, without excessive over-complication.

The basic idea is to rewrite the equations for $\rho'(r)$ and $m'(r)$ in terms of dimensionless (compact) variables and perform an analysis of the fixed points. The corresponding eigenvalues and eigenvectors obtained by linearising about these fixed points give a complete description of the nearby behaviour (Hartman-Grobman theorem, [21]) on the new state space, which can then be translated back to the physical picture by inverting the transformations given below. Interestingly, for the perfect fluid stars, the dependence of the total mass (as well as other quantities, e.g. the entropy) on the central density, ρ_0 , is governed by the behaviour around (and hence the eigenvalues of) a single fixed point. Specifically for our case we will see how this gives both an exact value for the critical dimension d_c , and a clear analytical explanation for the observed behaviour in the two regimes $d < d_c$ (oscillatory) and $d > d_c$ (monotonically increasing). We will also obtain expressions for the β_d and ν_d parameters introduced earlier.

To proceed, we thus set $R = \infty$, and our equations (9) and (10) become:

$$\rho'(r) = -\frac{\rho(r) d ((d-3)(d-2)(d-1)m(r) + 2r^{d-1}\rho(r))}{2(d-2)(d-1)(r^{d-2} - r m(r))} \quad (15)$$

$$m'(r) = \frac{2}{d-2} \rho(r) r^{d-2} \quad (16)$$

where $8\pi G_d$ has again been set equal to one. Note that we do not include the $d = 3$ scenario here as it is a special case (due to the non-dynamical nature of gravity). We can now introduce the dimensionless variables:

$$u = \frac{2r^{d-1}\rho(r)}{(d-2)m(r)} \quad (17)$$

and

$$v = \frac{(d-1)m(r)}{2r^{d-3}} \left(1 - \frac{m(r)}{r^{d-3}}\right)^{-1} \quad (18)$$

which allow equations (15) and (16) to be rewritten in the form:

$$\frac{du}{d\xi} = -u \left(1 - d + u + \left(d - 3 + \frac{u}{d-1}\right) \left(\frac{v d}{d-1}\right)\right) \quad (19)$$

$$\frac{dv}{d\xi} = -v \left(d - 3 - u + (d - 3 - u) \left(\frac{2v}{d-1}\right)\right) \quad (20)$$

where we have also introduced the new independent variable $\xi = \ln(r)$. For the case of positive mass and density we're considering here, both u and v are greater than zero (for non-zero r), and we make a final change of variables to the bounded U and V defined by⁷:

$$U = \frac{u}{1+u}, \quad V = \frac{v}{1+v} \quad (21)$$

which gives the system of equations:

$$\frac{dU}{d\lambda} = U(1-U) \left(d-1-dU - \left(2d-4 + \frac{d-3}{d-1} \right) V + \left(2d-3 + \frac{d(d-5)+3}{(d-1)^2} \right) UV \right) \quad (22)$$

$$\frac{dV}{d\lambda} = V(1-V)(3-d+(d-2)U) \left(1 + \left(\frac{2}{d-1} - 1 \right) V \right) \quad (23)$$

where we have also introduced the independent variable λ , defined by:

$$\frac{d\lambda}{d\xi} = \frac{1}{(1-U)(1-V)} \quad \left(= (1+u)(1+v) \right) \quad (24)$$

The fixed points of the system ((22) and (23)) are calculated in the usual fashion, by setting both $dU/d\lambda$ and $dV/d\lambda$ to zero and solving for U and V ; there are six in total, with eigenvalues then obtained from

$$\frac{d}{d\lambda} \begin{pmatrix} U \\ V \end{pmatrix} = \begin{pmatrix} \frac{\partial}{\partial U} \left(\frac{dU}{d\lambda} \right) & \frac{\partial}{\partial V} \left(\frac{dU}{d\lambda} \right) \\ \frac{\partial}{\partial U} \left(\frac{dV}{d\lambda} \right) & \frac{\partial}{\partial V} \left(\frac{dV}{d\lambda} \right) \end{pmatrix} \bigg|_{fp} \begin{pmatrix} U - U_{fp} \\ V - V_{fp} \end{pmatrix} \quad (25)$$

where the matrix components are evaluated at the particular fixed point under consideration. A table of such eigenvalues is given in [11], where they are labelled T_1, \dots, T_6 ; we do not list them all again here, however, as orbits in the interior of the state space $[0, 1]^2$ originate from either T_2 or T_4 and converge to the fixed point T_3 (as is shown in [13]). This fixed point corresponds to the singular self-similar solution given by equation (2.14) of [11], and due to the scale invariance of the system one can consider the entire set of (positive mass) solutions as being represented by a single orbit from T_2 to T_3 (this is true for any linear equation of state, $P(r) = q\rho(r)$).

Although one cannot write an analytic expression for this orbit, one can obtain approximations by linearising about the fixed points. As discussed briefly earlier, as this zero-cosmological constant solution is singular, in order to produce finite mass solutions the radiation must be confined to an (unphysical) box; the two fixed points T_2 and T_3 thus represent solutions with $\rho_0 = 0$ and in the limit $\rho_0 \rightarrow \infty$ respectively. The behaviour described by the linearisation about T_3 then reveals aspects of the large ρ_0 limit of the radiating stars (where the confining AdS potential results in

⁷Although the range of both U and V is defined as being $(0, 1)$, in order to perform the fixed point analysis of the asymptotic behaviour, it is necessary that the boundary points also be included; this requires the system given by (22) and (23) be \mathcal{C}^1 on $[0, 1]^2$, which is manifestly so.

the finite mass solutions without the need for any unphysical box), exactly what we analysed numerically in sections 3.2 and 3.3. This linearisation gives an explanation for the existence of a critical dimension and the differing behaviour seen in higher and lower dimensions, including quantitative expressions for d_c and the β_d and ν_d parameters of Table 1, as we shall now show.

Fixed point T_3 corresponds to the following values of U and V :

$$U_{T_3} = \frac{d-3}{d-2}, \quad V_{T_3} = \frac{2(d-1)^2}{2-4d+(d-1)d^2} \quad (26)$$

and has eigenvalues:

$$\begin{aligned} T_3^\pm &= \frac{d(d-3)}{2-4d+(d-1)d^2} \left(1-d \pm \sqrt{\frac{(d-12)d^2+13d-18}{d-2}} \right) \\ &\equiv k_d \left(1-d \pm \sqrt{\frac{(d-12)d^2+13d-18}{d-2}} \right) \end{aligned} \quad (27)$$

where we denote the coefficient k_d and observe that it is strictly positive for $d > 3$. These eigenvalues govern the behaviour of the solution, and we immediately see that there are two distinct regimes; one where the expression inside the square root is negative, corresponding to the oscillatory behaviour seen in figure 2, and one where the expression is positive, resulting in the monotonic behaviour seen in figure 3.⁸ We thus obtain a value for the critical dimension given by the solution to:

$$(d_c - 12)d_c^2 + 13d_c - 18 = 0 \quad (28)$$

which yields $d_c = 10.964\dots$, complementary to the value of $d_c = 11.0$ obtained numerically, although with the significance of being non-integer rather than exactly 11; interestingly for any linear equation of state the value of d_c is always in the range $10 \leq d_c \leq 11$, see [11].

We can relate the asymptotic behaviour obtained from the state space picture to the physical quantities of mass and density via several auxiliary equations to those given above, specifically:

$$\frac{dr}{d\lambda} = (1-U)(1-V)r, \quad \frac{dm}{d\lambda} = U(1-V)m \quad (29)$$

and

$$\frac{d\rho}{d\lambda} = -\frac{V}{d-1} \left(1-U + \frac{U}{d-1} \right) \rho \quad (30)$$

Given expressions for U and V in terms of λ (as obtained from an analysis of the behaviour around the fixed points, say), one can integrate the above to determine

⁸The fact that $k_d > 0$ ensures that the fixed point T_3 is a stable focus for the oscillatory behaviour in the $d < d_c$ case; for $d > d_c$, we have that T_3^\pm is strictly less than zero, and hence acts as a stable node.

corresponding expressions for the mass, radius and density in terms of λ . There is, however, a simple way to see the dependence of the total mass M_d on the central density ρ_0 , which also reveals the origin of the β_d and ν_d parameters of our numerical model in section 3.3.

Focusing then on the case where $d < d_c$, how does the imaginary term in (27) lead to the (self-similar) oscillatory behaviour manifest in the total mass at large ρ_0 ? This can be seen directly from the linearisation about T_3 , where we observe similar oscillations in the expressions for $U(\lambda)$ and $V(\lambda)$ (see below); as mentioned above, it is the behaviour around T_3 that governs the behaviour of the physical quantities in the large ρ_0 limit. By considering the behaviour of $U(\lambda)$ and $V(\lambda)$ in terms of ρ_0 , we can extract the coefficients which should then match those in (14) (as argued more fully in [13]). The solutions of (22) and (23) in the large λ limit (i.e. about the fixed point T_3) can be expressed as:

$$\text{Re}(U(\lambda)) = U_{T_3} + \exp(-(d-1)k_d\lambda) \cos\left(k_d\lambda\sqrt{\frac{18-(d-12)d^2-13d}{d-2}}\right) \quad (31)$$

$$\text{Re}(V(\lambda)) = V_{T_3} + \exp(-(d-1)k_d\lambda) \cos\left(k_d\lambda\sqrt{\frac{18-(d-12)d^2-13d}{d-2}}\right) \quad (32)$$

where we have only kept the real angular term as we are only interested in the period of the oscillations (ν_d) and the coefficient of the damping (β_d); the extra factors (namely α_d and μ_d) cannot be extracted directly from this analysis.⁹

For sufficiently high density stars (i.e. with large ρ_0), we have $\lambda \propto \frac{1}{2} \frac{d\lambda}{d\xi} \Big|_{T_3} \log(\rho_0)$, and we thus obtain:

$$\beta_d = \frac{(d-1)k_d}{2(1-U_{T_3})(1-V_{T_3})} = \frac{d}{4} + \frac{1}{2d} - \frac{3}{4} \quad (33)$$

and

$$\begin{aligned} \nu_d &= \frac{k_d}{2(1-U_{T_3})(1-V_{T_3})} \sqrt{\frac{18-(d-12)d^2-13d}{d-2}} \\ &= \frac{1}{4d} \sqrt{(d-2)(18-(d-12)d^2-13d)} \end{aligned} \quad (34)$$

which give the values shown in Table 2, provided as a comparison to the numerical estimates obtained in section 3.3. We see that they match very closely, with any discrepancies most likely due to a combination of numerical imprecision in the original data for the mass at large ρ_0 and the use of oscillations at insufficiently large ρ_0 for the asymptotic dependence to be totally dominant.

⁹Technically, for a solution of this form one should first make a linear change of coordinates such that the matrix on the RHS of (25) is in diagonal form. This only manifests itself, however, as extra multiplicative constants which do not affect the decay term β_d or oscillation period ν_d , and hence can be ignored.

d	β_d	ν_d
3.1	$231/1240 \approx 0.186$	$\sqrt{695519}/1240 \approx 0.672$
4	$3/8 = 0.375$	$\sqrt{47}/8 \approx 0.857$
5	$3/5 = 0.6$	$2\sqrt{6}/5 \approx 0.980$
6	$5/6 \approx 0.833$	$\sqrt{13/3}/2 \approx 1.04$
7	$15/14 \approx 1.07$	$2\sqrt{215}/5 \approx 1.05$

Table 2: Exact values (alongside decimal equivalents) obtained from the dynamical systems analysis for β_d and ν_d for the model of the total mass (14).

5 Discussion

What we have seen in the above analysis is firstly the appearance of a critical dimension ($d_c = 11.0$) from the simple requirement of a stability condition on our perfect fluid model for a gas of radiation, and a numerical study of the behaviour in various dimensions. Whilst the appearance of oscillations in the variation of the total mass with the central density ρ_0 in the lower dimensional cases had been noted before, we saw here that such oscillations do not appear to persist in the higher dimensional cases (see figures 2 and 3). Not only do the oscillations die down as the dimensionality is increased, by analysing the progression of the saturation point, ρ_c , we find that they disappear completely for d above a certain value. Although this value was calculated to be 11.0 in the original numerical analysis, the dynamical systems approach which followed in section 4 not only gave a more precise, non-integer value ($d_c = 10.964\dots$, as first derived in [11]), but also explained analytically why one sees a change from oscillatory to monotonic behaviour as one increases the dimension past this point. The section concluded by demonstrating how the β_d and ν_d parameters of the numerical model could also be derived via this analytical approach.

What is remarkable is that from a seemingly basic condition (that of monotonicity in the variation of the total mass), one arrives at such a simple relation for the dependence of ρ_c on d , namely equation (11). Such simplicity could not have been expected given the complex nature of the initial setup, which allows the spacetimes in question to be generated only numerically from the coupled ODEs. The extensions [4, 5, 6] to the BKL work on modelling a gravitational field close to a spacelike singularity also reveal a critical dimension of eleven.¹⁰ In their work they found that the general behaviour of the relevant Einstein solutions changed from “chaotic” in the low dimensional cases ($d < 11$) to non-chaotic in higher dimensions ($d \geq 11$), in

¹⁰Briefly, their analysis of the setup was performed using the mixmaster model, where the dynamical behaviour is governed by Kasner exponents and conditions upon them, and in which the evolution continues until the system reaches a stability region where the Kasner exponents remain constant. They observed that such a stability region could only exist for $d \geq 11$, and thus the evolution continues indefinitely for any lower number of dimensions. This has interesting consequences not elaborated on here, which are discussed in detail in the papers cited above.

much the same manner as we observe the transition from oscillatory to monotonic total mass behaviour in the radiating star case considered here. It is interesting that their work also reveals a critical dimension of eleven, and a more detailed comparison of the two different scenarios (including an analysis to determine the exact (possibly non-integer) value of d_c for their transition) may yield further insight.

It would be interesting to see if such a result appears in other investigations into scenarios similar to the radiating perfect fluid model considered here. For example, one could examine other physical equations of state to see if they exhibit the same behaviour, and indeed the work of [11] and [12] has pursued this idea further (see the note below). Finally, one could also look to explain the linear $d/2$ term which appears in (11), and whether there is any physical explanation for why the coefficient should take on the value of a half.

Note

Unknown to the author, this phenomenon has also been simultaneously investigated in two other works. In [11], Vladislav Vaganov analyses the behaviour of radiating perfect fluid models in d -dimensional AdS spacetimes; he notes (as we do here) that there is a significant change in the behaviour of the total mass for $d > 11$ (where it becomes a monotonic rather than oscillatory function of the central density), and demonstrates this not only for the mass but also the temperature and entropy.

He also presents a dynamical systems analysis (based on that given in [13]) of the behaviour for a general linear equation of state, $P(r) = q\rho(r)$, which includes the radiation case. This analysis complements the numerical results presented here, providing an analytic derivation of the critical density, which is determined to be $d_c = 10.964\dots$, consistent with our relation (11). The specific analysis for the radiation case is given in section 4, where we give not only the derivation of the critical density, but also demonstrate how the dynamical systems technique gives analytical expressions for other parameters introduced in our numerical investigation into the self-similar behaviour for $d < d_c$.

The second related paper, [12] by Pierre-Henri Chavanis, presents an in-depth study of the behaviour of general stars (“isothermal spheres”) with a linear equation of state in an asymptotically flat background. His results are again complementary, finding that there is monotonic behaviour for $d \geq 11$, in contrast to the oscillatory behaviour observed in lower dimensions. By asymptotic analysis he also finds the value for the critical dimension in the radiation case to be very close to eleven, and although there initially appeared to be a discrepancy between the two alternative calculations of the critical dimension in [11] and [12], the latter was subsequently corrected to agree with the value of $d_c = 10.964\dots$ found in [11]. His paper also includes a comprehensive investigation into the stability of the different regimes, looking at a number of alternative stellar configurations and considering the behaviour of other thermodynamic parameters (entropy, temperature, \dots), in addition to the mass.

Acknowledgements

I'd like to thank Veronika Hubeny for useful discussions and ideas, and Don Page for his comments which helped motivate this work, which was supported by an EPSRC studentship grant and the University of Durham Department of Mathematical Sciences.

References

- [1] R. Gregory and R. Laflamme, “*Black strings and p-branes are unstable*”, Phys. Rev. Lett. **70**, 2837 (1993) [arXiv:hep-th/9301052].
- [2] R. Gregory and R. Laflamme, “*The instability of charged black strings and p-branes*”, Nucl. Phys. B **428**, 399 (1994) [arXiv:hep-th/9404071].
- [3] V. A. Belinsky, I. M. Khalatnikov and E. M. Lifshitz, “*Oscillatory approach to a singular point in the relativistic cosmology*”, Adv. Phys. **19**, 525 (1970).
- [4] J. Demaret, M. Henneaux and P. Spindel, “*Non-oscillatory behaviour in vacuum Kaluza-Klein cosmologies*”, Phys. Lett. B **164**, 27 (1985).
- [5] J. Demaret, J. L. Hanquin, M. Henneaux, P. Spindel and A. Taormina, “*The Fate of the Mixmaster Behaviour in vacuum Inhomogeneous Kaluza-Klein Cosmological Models*”, Phys. Lett. B **175**, 129 (1986).
- [6] Y. Elskens and M. Henneaux, “*Chaos in Kaluza-Klein models*”, Class. Quant. Grav. **4**, 161-167 (1987).
- [7] T. Kaluza, “*On the problem of unity in physics*”, Sitzungsber. Preuss. Akad. Wiss. Berlin (Math. Phys.) 966-972 (1921).
- [8] J. M. Maldacena, “*The large N limit of superconformal field theories and super-gravity*”, Adv. Theor. Math. Phys. **2**, 231 (1998) [Int. J. Theor. Phys. **38**, 1113 (1999)][hep-th/9711200].
- [9] O. Aharony, S. S. Gubser, J. M. Maldacena, H. Ooguri and Y. Oz, “*Large N field theories, string theory and gravity*”, Phys. Rept. **323**, 183 (2000) [arXiv:hep-th/9905111].
- [10] V. E. Hubeny, H. Liu and M. Rangamani, “*Bulk-cone singularities and signatures of horizon formation in AdS/CFT*”, JHEP **0701**, 009 (2007) [arXiv:hep-th/0610041].
- [11] V. Vaganov, “*Self-gravitating radiation in AdS(d)*”, arXiv:0707.0864
- [12] P. H. Chavanis, “*Relativistic stars with a linear equation of state: analogy with classical isothermal spheres and black holes*”, arXiv:0707.2292

- [13] J. M. Heinzle, N. Rohr and C. Uggla, “*Spherically Symmetric Relativistic Stellar Structures*”, Class. Quant. Grav. **20** (2003) 4567 [arXiv:gr-qc/0304012].
- [14] R. Sorkin, “*A Criterion for the onset of instability at a turning point*”, Astrophys. J. **249**, 254-257 (1981).
- [15] H. A. Buchdahl, “*General Relativistic Fluid Spheres*”, Phys. Rev. **116** 1027-1034 (1959).
- [16] J. M. Heinzle, “*Bounds on $2m/r$ for static perfect fluids*”, arXiv:0708.3352
- [17] M. Abramowicz, I. Bengtsson, V. Karas, K. Rosquist, “*Poincare ball embeddings of the optical geometry*”, Class. Quant. Grav. **19** 3963-3976 (2002) [arXiv:gr-qc/0206027].
- [18] D. N. Page and K. C. Phillips, “*Self-gravitating radiation in anti-de Sitter space*”, GRG Vol. 17, No. 11 pp. 1029-1041 (1985).
- [19] C. Sire and P. H. Chavanis, “*Thermodynamics and collapse of self-gravitating Brownian particles in D dimensions*”, Phys. Rev. **E 66** (2002) 046133 [arXiv:cond-mat/0204303].
- [20] J. Hammersley, “*Numerical metric extraction in AdS/CFT*”, arXiv:0705.0159
- [21] P. Hartman, “*Ordinary Differential Equations*”, Birkhäuser, Boston (1982). For an introduction to dynamical systems, see J. D. Crawford, “*Introduction to bifurcation theory*”, Rev. Mod. Phys. **63** 4, 991-1038 (1991).